Materials Characterization 120 (2016) 124–128

Contents lists available at ScienceDirect

Materials Characterization

journal homepage: www.elsevier.com/locate/matchar

# Surface nanocrystallization of Mg-3 wt.% Li-6 wt.% Al alloy by surface mechanical attrition treatment

Lehao Zhang [a], Yun Zou [c], Hongtao Wang [b], Liang Meng [a], Jiabin Liu [a,*], Zhongwu Zhang [c,*]

[a] School of Materials Science and Engineering, Zhejiang University, Hangzhou 310027, China
[b] Institute of Applied Mechanics, Zhejiang University, Hangzhou 310027, China
[c] College of Materials Science and Chemical Engineering, Harbin Engineering University, Harbin 150001, China

ARTICLE INFO

*Article history:*
Received 22 March 2016
Received in revised form 5 July 2016
Accepted 17 August 2016
Available online 19 August 2016

*Keywords:*
Magnesium-lithium alloy
Surface mechanical attrition treatment
Grain refinement
Nanoindentation
Transmission electron microscope

ABSTRACT

A nanocrystalline surface layer was produced on Mg-3 wt.% Li-6 wt.% Al alloy by means of surface mechanical attrition treatment (SMAT). Microstructure features of various sections were systematically characterized by transmission electron microscopy. The results indicate that grain refinement induced by SMAT is dominated mainly by dislocation slip. Twinning is active at the early stage of grain refinement process when the grain size is large. The dislocation-dominated deformation mechanism is attributed to the change of *c*/*a* ratio due to the alloying of Li in Mg matrix and the suppression of twinning due to grain refinement. Nanoindentation results show that the hardness of the surface is enhanced by SMAT.



## 1. Introduction

Magnesium-lithium (Mg-Li) alloys are the lightest metallic materials with the density of ~1.35–1.65 g/cm$^3$ [1]. Due to the remarkable features of the ultra-lightness and improved formability, Mg-Li alloys are attracting more and more interests and promising to be applied in aerospace, transportation and communication industries [1]. Mg-Li alloys exhibit different crystal structures depending on the lithium content according to the phase diagram [2]. When the addition of lithium is <5 wt.%, the alloys are composed of magnesium solid solution with a hexagonal close-packed (hcp) structure (α phase). When the addition of lithium is higher than 11 wt.%, the alloys transfer to body-centered cubic structure (β phase). When the addition of lithium is between 5 and 11 wt.%, the alloys are composed of both α and β phases [3]. In general, Mg-Li alloys containing single α phase have higher strength than those containing single β phase, making them more favorable for applications in structural components [4]. Aluminum is an element with high solubility in Mg-Li alloys. The addition of Al in Mg-Li alloys improves the strength remarkably with only a slight increase in density [5]. The effects of Al alloying additions on the deformation behavior of extruded Mg-4 wt.% Li was studied by Lentz et al. [6], and they found that the increases in the yield stress and hardening rate with the addition of Al is a consequence of increases in the resistances to slip but a decrease in the resistance to $\{10\bar{1}2\}\langle 10\bar{1}\bar{1}\rangle$ twinning.

The design and optimization of mechanical properties of Mg-Li alloys have been extensively investigated. Alloying and deformation are two major ways to increase the mechanical properties of Mg-Li alloys. With 1 wt.% Sc addition in Mg-3 wt.% Li alloy, the yield strength increases from 158 MPa to 189 MPa [4]. With 2% wt.% RE addition in Mg-3.5 wt.% Li-2 wt.% Al alloy, the tensile strength increases from 100 MPa to 175 MPa [7]. Equal channel angular pressing can enhance the yield strength of Mg-3.3 wt.% Li from 69 MPa to 113 MPa [8]. The alloys after extrusion have better mechanical properties than those after rolling as for Mg-8 wt.% Li-(0–3) wt.% Ce alloys [9]. When increasing the extrusion ratio, the strength was enhanced while the ductility was decreased [10].

In most cases, materials failure occurs on their surface, such as fatigue fracture, wear and friction [11]. These failures are sensitive to the structure and properties of the material surface. So it is necessary to improve the surface properties of materials, such as hardness. There are many ways to enhance surface hardness, among which surface mechanical attrition treatment (SMAT) is one of the most effective methods [12]. By means of severe plastic deformation, the grain size on the surface of a conventional bulk material can be reduced down to nanometer scale. This kind of surface modification will greatly enhance the surface properties without changing the chemical composition [12].

* Corresponding authors.
*E-mail addresses:* liujiabin@zju.edu.cn (J. Liu), zwzhang@hrbeu.edu.cn (Z. Zhang).

http://dx.doi.org/10.1016/j.matchar.2016.08.017
1044-5803/

In hexagonal close-packed Mg base alloys, strain along the ⟨0001⟩ axis can be accommodated only by twinning and $\frac{1}{3}<11\bar{2}3>$ slip [13]. Recently, it was suggested that higher activation of non-basal slip might be responsible for the deformation in Mg-Li base alloys [6]. Zou et al. [14] also investigated the deformation modes transition in α phase of the duplex Mg-9 wt.% Li alloy with various thickness reductions, and they concluded that the activation sequence of deformation modes is basal slip first, and then pyramidal slip during hot-rolling to a thickness reduction of 40%. The relative activity of <c + a> slip decreases with further thickness reduction. However, it is not well understood that how the deformation twinning and dislocation activation in Mg-Li base alloys affect the grain refinement mechanism during SMAT. In this study, the microstructure evolution, specifically surface nanocrystallization of Mg-3 wt.% Li-6 wt.% Al alloy during SMAT and their effects on hardness are investigated systematically. An unexpected microstructure refinement mechanism is found and discussed based on the change of crystal structure.

## 2. Experimental procedure

The material used in this study is Mg-3 wt.% Li-6 wt.% Al alloy (LA36). The alloy was prepared by melting high purity magnesium (99.9%), lithium (99.9%), and aluminum (99.9%) in a vacuum induction furnace with argon atmosphere protection and then cast into a copper mold. The ingots with dimensions of about 150 mm × 120 mm × 35 mm were rolled to sheet with a reduction of 40% at 300 °C.

The SMAT set-up and procedures have been described in detail elsewhere [15]. In this work, a vibration frequency of 20 kHz and stainless steel balls of 3 mm in diameter were selected, and the LA36 samples with a thickness of about 1 mm were treated at room temperature for 1 min, 10 min and 30 min, respectively. Both sides of the sample were conducted alternately under nitrogen shielded atmosphere protection.

The microstructure characterization was performed by transmission electron microscope (TEM) on JEM-2100 operated at 200 kV. The plane-view thin foils for TEM were prepared by mechanical grinding, followed by thinning via Gatan PIPS. The TEM specimens for settled depth were prepared by focus ion beam using the standard lift-out techniques in a FEI Quanta 3D. The specimens for optical microscopy observation were polished and etched with 4 vol.% nital. The measurements of hardness along the depth of the cross-section were performed by the Agilent Technologies Nano Indenter G200 with a Berkovich diamond indenter. The nanoindenter was calibrated by using a $SiO_2$ standard specimen and the distance between any two neighboring indentations was at least 50 μm. X-ray diffraction (XRD) tests were carried out in a LabX XRD-6000 using Cu Kα radiation.

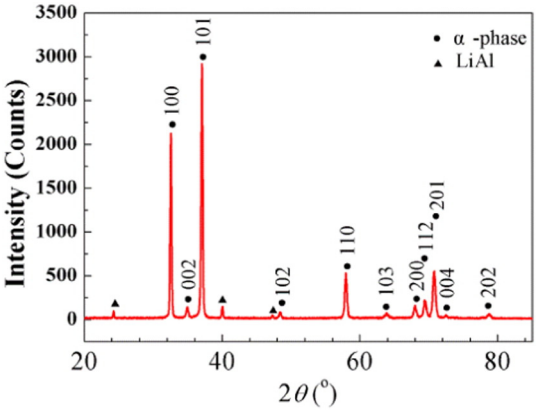


**Fig. 1.** XRD pattern of LA36 before SMAT.

## 3. Results and discussion

The XRD pattern of the LA36 is illustrated in Fig. 1. The XRD result confirms that the LA36 mainly consists of α-Mg and a little LiAl phase. The peaks from α-Mg shift to high angle with respect to standard Mg peaks due to the substitution of Mg atoms by Li and Al atoms. The lattice parameters *c* and *a* of pure magnesium are 0.320936 nm and 0.52112 nm, respectively, with a *c*/*a* ratio of 1.6238 [16]. In this study, the *c* and *a* of LA36 measured by XRD are 0.31760 nm and 0.51416 nm, respectively, with a *c*/*a* ratio of 1.6189. This indicates that the solid solution of Li and Al in Mg decreases the *c*/*a* ratio of Mg-Li base alloy.

Fig. 2 shows the typical TEM observation of the top surface layer after 10 min treatment. Clearly, a nanostructured surface layer is developed. The corresponding selected area electron diffraction (SAED) patterns in Fig. 2(a) indicate that the nanograins are highly disoriented with respect to each other. Fig. 2(b) and (c) are the dark-field TEM images corresponding to the "b" and "c" circles in Fig. 2(a), respectively. The nano-sized grains are clearly outlined in the dark-field TEM images. Fig. 2(d) indicates that the majority of the grain size on the top surface is smaller than 100 nm and the average grain size is about 80 nm. The grain size was measured from a single bright field TEM image along with several dark field TEM images (at least four) in order to determine the size of each grain with greater precision.

The microstructure evolution during SMAT is shown in Fig. 3. As can be seen from Fig. 3(a), the initial grain size of LA36 is about 40 μm. The grain size decreases to ~5 μm, 80 nm and 80 nm, respectively, after SMAT for 1 min, 10 min and 30 min (Fig. 3(d)). It is found that the grain size could not be refined further after SMAT for 10 min. In other words, the grain size refinement of LA36 reaches its limit when the sample is SMATed for 10 min.

It is well known that the refinement of grains during SMAT is induced by the severe plastic deformation. In general, SMAT-affected surface layer can be divided into three regions from the top surface to matrix: the nanocrystalline region, submicrocrystalline region and deformed region [17]. Each region provides different microstructure information about strain-induced grain refinement process during SMAT. To investigate the mechanisms of the grain refinement, it is an effective way to tailor the microstructure evolution associated to various straining. For this purpose, systematic investigations on the microstructures at various depths from the top surface of the SMATed samples were carried out. Fig. 4 shows the typical bright field TEM images and corresponding SAED patterns at various depths from the top surface of the LA36 sample SMATed for 30 min. For the microstructure at about 500 μm depth, high density of dislocations are observed inside the grains while the grain size has little change (Fig. 4(a)). At about 300 μm depth, typical dislocation cellular structure is found with an extremely high dislocation density at the cell walls and relatively low inside cells (Fig. 4(b)). The size of dislocation cells is about 300 nm, which approaches the lower limit of conventional dislocation cell size [11]. The corresponding SAED patterns still show single crystal characteristic while the spots are expanded slightly, indicating that there is little misorientation across the dislocation cell walls. If the size of dislocation cells further reduces, the dislocation cells would lose stability and evolve into subgrains. Fig. 4(c) shows the subgrains in a depth of about 100 μm from the top surface. The subgrain characteristics are well confirmed by the corresponding SAED patterns showing typical rings. The grains are refined down to around 80 nm due to the high strain at the top surface as shown in Fig. 4(d).

Fig. 5(a) presents typical TEM micrographs showing the deformation twins in LA36 after SMATed for 30 min at a depth of about 300 μm. The SAED patterns in Fig. 5(b) show that the twin system is $\{1\,0\bar{1}2\}\langle 10\bar{1}1\rangle$. The twin interface is determined to be $(01\bar{1}2)$. Different with hcp structured pure magnesium [18] and pure titanium [19], the density of deformation twin in the SMATed LA36 is relatively low.